https://doi.org/10.1016/j.enconman.2020.113448

Multi-objective optimization and life cycle assessment of an integrated system combining $LiBr/H_2O$ absorption chiller and Kalina cycle

Nan Xie[a], Zhiqiang Liu[a, b], Zhengyi Luo[a], Jingzheng Ren[c], Chengwei Deng[d], Sheng Yang[a, *]

a. School of Energy Science and Engineering, Central South University, Changsha 410083, China

b. Collaborative Innovation Center of Building Energy Conservation & Environmental Control, Zhuzhou 412007, China

c. Department of Industrial and Systems Engineering, Hong Kong Polytechnic University, Hong Kong SAR, China

d. Space Power Technology State Key Laboratory, Shanghai Institute of Space Power-Sources, Shanghai 200245, China

*Corresponding author:

Sheng Yang

School of Energy Science and Engineering

Central South University, Changsha, 410083, P. R. China.

Tel: +86-731-88879863

E-mail address: ceshyang@csu.edu.cn

Abstract

Multi-objective optimization of an integrated waste heat recovery system combining absorption refrigeration cycle and Kalina cycle is investigated in present research. Life cycle assessment (LCA) is inserted into the multi-objective optimization model to evaluate the environmental performance. Eco-indicator 99 (EI99) method is used to translate eleven environmental impacts into a single criterion EI99. The proposed multi-objective optimization model includes three objective functions: thermal efficiency, annualized total cost (ATC) and EI99, from the energetic, economic and environmental (3E) aspects. Non-dominated sorting genetic algorithm II is employed to solve the conflicts among three objectives of this optimization model. Pareto optimal solutions are obtained, presenting the optimal trade-off among objectives. Technique for Order Preference by Similarity to an Ideal Solution and Shannon entropy approach are combined for decision making. Results show that the presented multi-objective optimization model properly handles the contradictions in this optimization problem. By using the combined decision-making technique, the final optimal solution is determined. This optimal scheme achieves around 9.34% and 9.53% higher thermal efficiency and EI99 at the cost of 3.03% higher ATC. Therefore, with sufficient consideration, this final optimal solution is superior to other solutions. LCA of this proposed system is then comprehensively conducted and compared with the individual KC. Comparison results indicate that this integrated system is obviously better than the individual KC from the environmental point of view. This research provides in-depth knowledge of the 3E performance analysis and multi-objective optimization of a cascade waste heat recovery process.

Keywords: multi-objective optimization; genetic algorithm; life cycle assessment; waste heat recovery; system integration

Nomenclature

C	cost
DAM	overall damage of damage category
dm	damage coefficient
f	correction factor
h	specific enthalpy, mass enthalpy (kJ/kg)
IMP	overall damage of impact category
i	interest rate
M	equipment cost exponent index
m	mass flow rate (kg/h)
n	operation year
n	normalization factor
P	pressure (kPa)
Q	heat flow rate (kW)
T	temperature (°C)
W	work or electrical power output (kW)
w	weighting factor
X	mass concentration (wt%)
x	abscissa
y	ordinate

Greek symbols

η	thermal efficiency
η_p	overall efficiency of pump
η_t	overall efficiency of turbine

Subscripts

A	absorption chiller
B	base cost
b	chemical b
build	buildings
cont	contingency
d	damage category
dec	design engineering and construction
E	equipment
elec	electrical
er	equipment erection
evap	evaporator
F	fixed cost
H	high temperature
inst	instrumentation and controls
K	Kalina cycle
L	low temperature
M	materials
os	off-sites
P	pressure
pip	pipe connection
r	impact category
sp	site preparation
T	temperature

util	utilities
ws	working capital

Abbreviations

ATC	annualized total cost
CEPCI	Chemical Engineering Plant Cost Index
COP	coefficient of performance
DALY	Disability-Adjusted Life Years
EI99	Eco-indicator 99
GWP	Global warming potential
HTR	high-temperature recuperator
KC	Kalina cycle
LCA	life cycle assessment
LCI	life cycle inventory
LiBr	lithium bromide
LTR	low-temperature recuperator
NO_X	nitrous oxides
NSGA-II	Non-dominated sorting genetic algorithm II
ORC	organic Rankine cycle
PDF	potentially disappear fraction
TOPSIS	Technique for Order Preference by Similarity to an Ideal Solution

1. Introduction

Kalina cycle (KC) is a promising waste heat recovery technology for electric power production. Ammonia concentration of the working medium decreases because ammonia vapor tends to escape from the solution when heated, leading to a temperature/concentration changing heat transfer process [1]. Four configurations of power generation cycles were investigated in a temperature range from 98 to 162 °C [2]. In terms of max electricity output, economic performance, energetic and exergetic efficiencies, the Kalina cycle was recommended as a viable choice. System integration is seen as an effective way to improve the process efficiency and economic performance, and also to alleviate the environmental impacts [3]. A combined system of KC and ejector refrigeration cycle was investigated by Rashidi and Yoo [4]. Through an optimization from the exergy and pinch analyses, the thermal, power-cooling and exergetic efficiencies were improved by 32%, 36% and 32%. A novel cogeneration heating system was adopted to recover the condensed waste heat. Compared with conventional cogeneration cycles, this novel system has higher exergy efficiency, lower equivalent electricity of heating and lower heating cost [5]. Absorption refrigeration system can also re-utilize low-grade waste heat with advantages such as low electricity consumption, low maintenance cost and environmental friendliness [6, 7]. A solar driven absorption-compression refrigeration cycle was studied from energetic, exergetic, economic and environmental aspects [8]. Single-/double- effect absorption chiller/KC coupled systems have also been studied and compared [9, 10]. Lithium bromide (LiBr) is a non-toxic and non-flammable substance and it works with a relatively low working pressure [11]. Rashidi et al. [12] compared a NH_3/H_2O absorption chiller/KC integrated system with a $LiBr/H_2O$ absorption chiller/KC system in terms of energetic and economic performance [13]. A solar driven $LiBr/H_2O$

absorption refrigeration system was proposed [14] and this coupled system recovers the extra heat of solar cells to produce electricity. A LiBr/H_2O absorption chiller was inserted into a concentrating photovoltaic/KC coupled system [15]. The absorption chiller absorbs the waste heat of solar cells to achieve higher electricity production in comparison with the individual KC.

Investigating the effects of operational parameters in a certain system relies on a parametric analysis of this system. While reasonable system optimization is still not easy to be achieved without knowing the optimal combination of these parameters. Multi-objective optimization is critical in developing various industrial systems in which there are many operational parameters and process integration [16]. Multi-objective optimization of a catalyzed batch transesterification process was conducted using Orthogonal collocation on finite elements method, to obtain the highest concentration of fatty acid methyl esters [17]. Multi-objective optimization of an organic Rankine cycle (ORC)/absorption chiller was carried out by using Multi-objective particle swarm optimization algorithm [18]. Multi leader multi-objective particle swarm optimization algorithm was utilized in a solar driven NH_3/H_2O absorption cooling system [19], to simultaneously achieve the highest coefficient of performance (COP) and exergy efficiency in both chiller and solar system and the lowest annual capital cost. θ-dominance based evolutionary algorithm was adopted to solve the economic emission dispatch problem in combined heat and power system [20]. An integrated gasification combined cycle (IGCC), a membrane unit and a supercritical Rankine cycle were combined to produce hydrogen and electricity at the same time [16]. Artificial neural network and genetic algorithm were integrated to achieve the optimal performance in terms of energetic and exergetic efficiencies, production cost of hydrogen and electricity. Genetic algorithm, inspired by natural evolution theory,

consists of four steps including initialization, selection, crossover and mutation. It is an evolutionary algorithm for searching optimal solutions of engineering problems [21]. Series and parallel absorption chillers were studied using genetic algorithm to solve the contradictions among system COP, exergetic performance and system irreversibility [21]. Multi-objective optimization of single-, double- and triple-effect $LiBr/H_2O$ absorption chillers was carried out using genetic algorithm, to minimize the energy consumption and economic cost [22]. Conflicts between the economic and thermodynamic performance of a cascade absorption refrigeration was also investigated [23]. A molten carbonate fuel cell, a gas turbine and an ORC were coupled and studied considering conflicting objectives of exergetic and economic performance [24]. For environmental evaluation, the penalty cost due to emissions of CO, NO_x and CO_2 was considered in the total expenditures. Non-dominated sorting genetic algorithm II (NSGA-II), with less computational complexity, is a common tool for solving multi-objective problems. Conflicts between thermodynamic and economic performance in a $LiBr/H_2O$ absorption heat transformer were studied and then optimized using NSGA-II algorithm [25]. A micro gas turbine, a steam generator, an ORC and a multi-effect desalination cycle were combined with the distilled water production and power generation cost being selected as objectives [26]. Refinery off-gas and natural gas were simultaneously fed into a coupled hydrogen production system to realize the max production of hydrogen and steam [27]. An improved NSGA-II technique was used to minimize the operation and environment cost in an integrated energy system combining wind turbine, photovoltaic cell, electrolytic hydrogen, fuel cell and hydrogen storage [28]. From the literature review, there are many available optimization methods for various multi-objective optimization problems. NSGA-II has a low computational complexity by using the non-dominated sorting. Introducing the elitism strategy ensures

197 the good individuals will not be lost so as to improve the results accuracy. Diversity of
198 the population is guaranteed relying on the crowding distance sorting process.
199 Therefore, NSGA-II has become the most popular methods for many industrial multi-
200 objective optimization problems.

201 Life cycle assessment (LCA) is an assessment method for a certain industrial
202 system throughout its life cycle with consideration of inputs, outputs and environmental
203 impacts [29]. It is a valuable technique for presenting energetic and environmental
204 profile for certain product or process [30]. LCA of a solid waste management system
205 was conducted to minimize CO_2 production, energy consumption and to improve
206 economic performance [29]. However, LCA cannot provide alternatives for
207 performance and environmental improvements [31]. In an absorption refrigeration
208 cycle, LCA was coupled with the multi-objective optimization to reduce the annualized
209 total cost and environmental effects [31]. LCA was also inserted into a multi-objective
210 model for obtaining the optimal construction areas of rainwater harvesting systems [32].
211 A comprehensive evaluation of environmental and human health impacts was carried
212 out throughout the whole life cycle. Multi-objective optimization and LCA were also
213 conducted in solar driven absorption cooling and heating cogeneration systems [30]. To
214 make a full comparison, the adopted optimization approaches, advantages,
215 disadvantages and remarks of the published works are summarized in Table 1.
216

217

Table 1 Comparisons among published literature.

No.	System	Optimization method	Advantages	Disadvantages	Remarks
[16]	IGCC/supercritical Rankine cycle	neural network genetic algorithm	hydrogen/electricity production	future research needed for more coal types no environmental consideration	effect of three coal types was studied, lower coal grade has less expensive hydrogen and electricity production
[17]	integrated biodiesel production and separation system	Orthogonal collocation on finite elements method	dynamic optimization	no environmental consideration	energy consumption of reactor is much higher than that of the distillation columns
[18]	integrated ORC/absorption chiller	Multi-Objective Particle Swarm Optimization algorithm	driven by geothermal energy energy/exergy/economic analysis	no environmental consideration	increases the energy efficiency decreases the exergy efficiency best electricity/cooling cost and exergy efficiency were obtained
[19]	ammonia-water absorption chiller	Multi Leader Multi-Objective Particle Swarm Optimization algorithm	driven by various solar collectors thermo-economic analysis	no environmental consideration the final solution depends on the designer decision	effects of various solar collector types were studied
[20]	combined heat and power system	θ-dominance based evolutionary algorithm	incorporation of the optimization method with fuzzy c-means clustering to determine the best compromise solutions	/	meet the needs under changing system operating conditions
[21]	double effect absorption chiller	genetic algorithm	optimization for lithium chloride-water and lithium bromide-water double effect absorption chiller	exergy efficiency and system irreversibility simultaneously used as objectives	lithium chloride-water system has lower COP, higher exergy efficiency and less irreversibility
[22]	LiBr-water absorption chillers	genetic algorithm	driven by solar energy single-, double-, and triple-effect Linear Programming Technique for Multidimensional Analysis of Preference decision-making method	/	government subsidies and incentives are required for the high capital cost of these systems
[29]	municipal waste management system	NSGA	life cycle assessment two-/three-objective optimization current and new technologies	the final solution depends on the designer decision	utilizing newer technologies has less cost, less CO_2 savings and less energy consumption

[30]	absorption cooling and heating systems	Weighted-Tchebycheff metric approach	driven by solar energy energy/economic/environmental analysis short computational time	decision is made according to users' preferences	performance measures and optimization model suitable for other renewable energy systems
[31]	absorption cooling systems	ε-constraint method	life cycle assessment environmentally conscious system	the final solution depends on the designer decision	provide a sustainable design of absorption chillers which cause less environmental effect
[23]	cascade absorption chiller	NSGA-II	low-grade waste heat recovery energy/exergy/economic analysis	no environmental consideration	generator and absorber have the priority for exergy performance improvement
[24]	integrated molten carbonate fuel cell/ORC	NSGA-II	energy, exergy, economic and environmental analysis	environmental performance is not considered in the optimization model	integration with the ORC leads to 5% improvement in the exergy efficiency of the proposed system
[25]	absorption heat transformer	NSGA-II	energy/exergy/economic analysis	no environmental consideration	lower condenser and absorber temperatures improve the overall energy and exergy performance but more expensive
[26]	integrated ORC/multi-effect desalination	NSGA-II	exergy and economic analysis working medium comparisons	environmental consideration was based on previous studies	higher compressor pressure ratio increases exergy efficiency and decreases the cost rate
[27]	integrated hydrogen production process	NSGA-II	internal refinery sources are used for hydrogen supply	no economic, exergy and environmental analysis	provides a method to achieve simultaneous max hydrogen production and steam output
[28]	integrated hydrogen storage energy system	NSGA-II	day-ahead power dispatching dynamic optimization strategy	dispatching plan is chosen by decision makers based on needs	the multi-objective optimization scheme reduces carbon emissions and operating cost
[32]	rainwater harvesting systems	NSGA-II	life cycle assessment sensitivity analysis	decision making method is not provided	optimal construction area was obtained, daily maximum precipitation is the key factor
[33]	biogas pressurized water scrubbing process	NSGA-II	plant-level optimizing control	no environmental consideration	system CO_2 removal rate is 99.8% for various disturbances

218

In our previous research, absorption refrigeration cycle and Kalina cycle have been integrated to re-utilize a specific waste heat [34]. Using the cooling output of absorption chiller to cool down the basic solution of Kalina cycle can increase the turbine expansion ratio, resulting in a higher electrical power generation. The integrated system has a 45% higher thermal performance comparing with the individual Kalina cycle, which indicates the system performance is greatly improved after the integration. Based on the literature review, the multi-objective optimization of the absorption chiller/KC integrated system has never been investigated for cascade waste heat recovery. Also, LCA of this waste heat recovery process has not been comprehensively studied. In this work, multi-objective optimization and life cycle assessment are combined to achieve the optimal energetic, economic and environmental (3E) performance of this integrated system. Thermal efficiency of energetic analysis, annualized total cost (ATC) of economic analysis and Eco-indicator 99 (EI99) considering environmental impacts are selected as three objective functions in the multi-objective optimization model. A series of Pareto points are obtained, presenting the optimal trade-off among the 3E performance. Main contributions of this research can be summarized as: (1) Multi-objective optimization problem of an absorption refrigeration cycle/Kalina cycle integrated system are investigated for cascade waste heat utilization; (2) Life cycle assessment is inserted into the multi-objective optimization model as the major environmental performance index; (3) Energetic, economic and environmental (3E) performance of the integrated system are studied at the same time; (4) NSGA-II algorithm, Technique for Order Preference by Similarity to an Ideal Solution (TOPSIS) and Shannon entropy approach are combined in the multi-objective optimization model. This work also provides in-depth knowledge of the absorption chiller/KC integrated system for cascade waste heat recovery.

2. System description

Fig. 1 depicts the absorption chiller/KC integrated system. The chiller works as the auxiliary cooling cycle of KC. These two cycles are driven by the high-temperature part and low-temperature part of a given waste heat. Processes in the power generation cycle are: 1) The basic solution (Stream K4) absorbs waste heat Q_H and turns into vapor (K5) and weak solution (K7); 2) The ammonia vapor (K5) flows into the turbine for electricity generation and the weak solution (K7) releases heat in High-temperature recuperator (HTR); 3) This cooled solution (K8) enters the valve and then flows into the mixer to absorb the exhaust stream (K6) from the turbine; 4) After the mixing process, the strong solution (K10) is cooled in another recuperator (Low-temperature recuperator, LTR) and the cooled solution (K11) is further cooled in the evaporator; 5) After a pumping process, this basic solution (K2) recovers heat in two recuperators and enters the generator for continuing operation. Processes in the absorption cycle are: 1) The dilute solution (A1) absorbs heat Q_L and turns into refrigerant vapor (A2) and concentrated solution (A6); 2) After cooling and throttling processes, the condensed refrigerant (A4) enters the evaporator to cool down the basic solution of KC (K11); 3) The concentrated solution (A6) releases heat in a heat exchanger and flows through a throttling valve; 4) Then, the refrigerant (A5) is absorbed in the absorber by the strong solution (A8); 5) The weak solution (A9) is pumped back to the generator for another cycle operation. The absorption chiller recovers the thermal energy with lower temperature, i.e. the waste heat from KC. Eventually, the waste heat recovery is achieved relying on this cascade process. Fig. 2 is the temperature-entropy diagram (T-S diagram) of the KC in the integrated system, providing a distinct expression of the power generation process from the thermodynamics aspect.

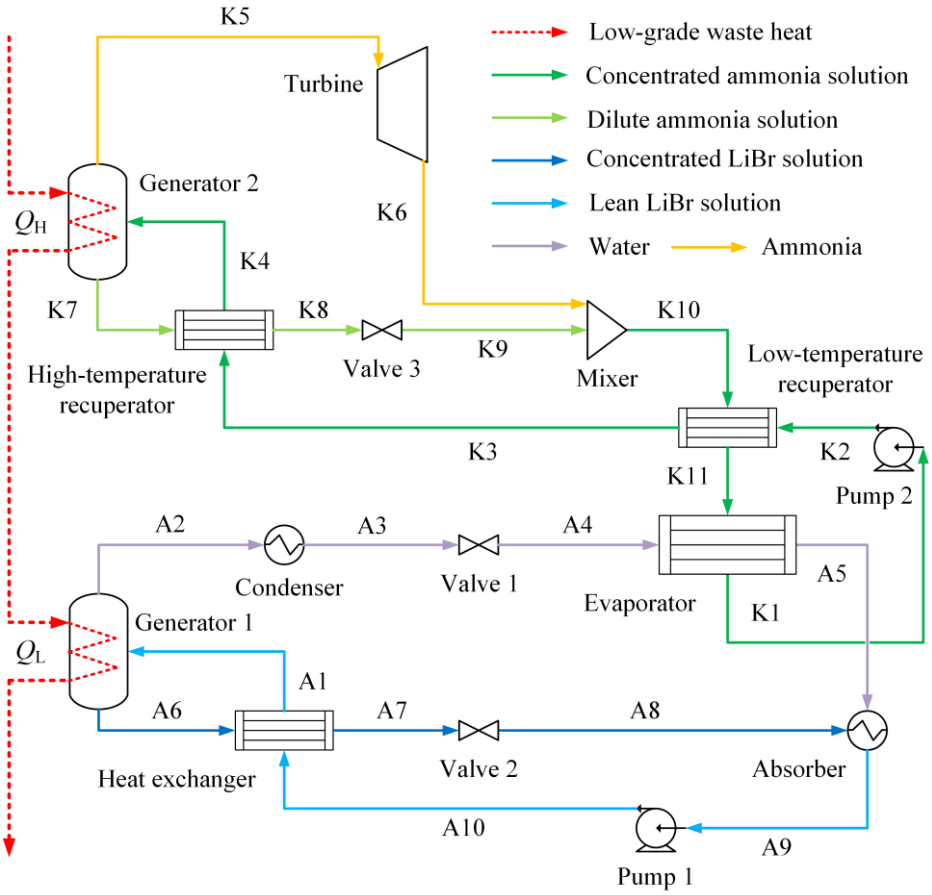

Fig. 1 Flowsheet of the integrated system.

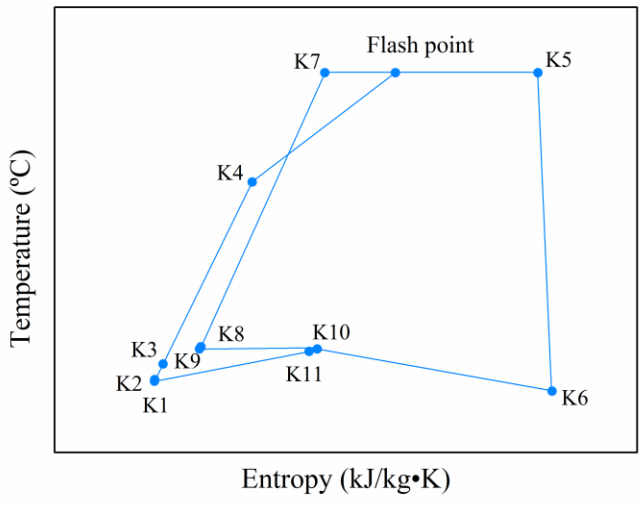

Fig. 2 T-S diagram of the KC in the integrated system.

3. Methodology

276 3.1 Parameter specifications and basic assumptions

277 A specific waste heat of 600 kW is given with temperature range of 90-150 °C. An
278 artificial temperature, segment temperature, divides the waste heat into two parts. The
279 KC generator temperature is assumed to be 10 °C lower than the segment temperature.
280 Generator temperature of the absorption chiller is 10 °C lower than the lower limit 90 °C.
281 Refrigeration temperature of the chiller is in the range of 2-10 °C. Cooling water is
282 assumed to have a temperature of 30 °C. The minimum temperature approach is 5 °C
283 in the absorber and condenser. Accordingly [1, 13, 15, 35-40], basic assumptions are
284 given as: (1) Steady state is assumed for the whole system; (2) Kinetic and potential
285 energy change is not considered; (3) No heat loss and pressure drop; (4) NH_3/H_2O
286 solution and $LiBr/H_2O$ solution at generator inlet/absorber outlet are saturated; (5) H_2O
287 vapor and NH_3 vapor at the generator outlet/absorber inlet are saturated; (6) Isentropic
288 efficiencies are assumed for turbine and pumps; (7) Leakage are neglected; (8)
289 Isenthalpic throttle valves. Aspen Plus software is utilized for process simulation of the
290 integrated system. Electrolyte pairs of ELECNRTL model for absorption chiller
291 simulation and binary parameters of PSRK model for KC simulation were obtained in
292 our previous research [41-43]. Table 2 presents the detailed block type selection and
293 settings for each equipment in the integrated system.

294 **Table 2** Block type and parameters specification.

Equipment	Block type	Specification
$LiBr/H_2O$ absorption refrigeration cycle		
Generator 1	Heater	Inlet heat stream, specified; Pressure drop, 0 kPa
	Flash2	Duty, 0 kW; Pressure drop, 0 kPa
Condenser	Heater	Vapor fraction, 0; Pressure drop, 0 kPa
Valve 1	Valve	Outlet pressure, specified
Evaporator (cold side)	Heater	Vapor fraction, 1; Pressure drop, 0 kPa
Absorber	Heater	Vapor fraction, 0; Pressure drop, 0 kPa
Heat exchanger	HeatX	Hot outlet-cold inlet temperature approach, 5 °C
Valve 2	Valve	Outlet pressure, specified
Pump 1	Pump	Discharge pressure, specified; Efficiency, 0.90
Kalina cycle		
Generator 2	Heater	Temperature, specified; Pressure drop, 0 kPa
	Flash2	Duty, 0 kW; Pressure drop, 0 kPa

Turbine	Turbine	Isentropic; Discharge pressure, specified; Isentropic efficiency, 0.88
Mixer	Mixer	Pressure drop, 0 kPa
High-temperature recuperator	HeatX	Hot outlet-cold inlet temperature approach, 5 °C
Valve 3	Valve	Outlet pressure, specified
Low-temperature recuperator	HeatX	Hot inlet-cold outlet temperature approach, 5 °C
Evaporator (hot side)	Heater	Temperature, specified; Pressure drop, 0 kPa
Pump 2	Pump	Discharge pressure, specified; Efficiency, 0.90

3.2 Validation

To validate the process simulation, simulation results were compared with published literature and a good agreement has been achieved [34]. The simulation results of absorption refrigeration cycle and Kalina cycle are validated separately. Table 3 shows the performance comparison between the absorption chiller in this work and the one in published work [44]. Table 4 gives the KC simulation results in this research and in published literature [15]. The present results are consistent with those in the published works. Therefore, the reliability of present simulation is guaranteed. Although this research is conducted based on reasonable specifications and assumptions. Leakage of working medium, pressure drop in devices and pipelines, heat dissipation, etc., are inevitable in practical systems. Besides, efficiencies of equipment would change with working conditions and steady state operation of system would be hard to achieve. Hence the operation status of the simulated system would have some differences with the real system. And the obtained results would also be different to some degree. Thus, pilot-scale tests of novel systems are always necessary before these systems are first put into operation.

Table 3 Comparison of absorption chiller COP between this work and published literature [44].

Parameter	Type	Literature results	Present results	Error (%)
Generator temperature (°C)	Input	85	85	/
Condenser temperature (°C)	Input	40	40	/
Absorber temperature (°C)	Input	110	110	/
COP	Output	0.470	0.468	0.4

Table 4 Comparison of KC simulation results between present work and published literature [15].

Stream No.	*T* (°C)		*P* (kPa)		*X* (wt%)		*m* (kg/h)	
	present	literature	present	literature	present	literature	present	literature
s1	19.6	20.0	470	470	0.70	0.70	132.76	132.76
s2	21.3	21.7	7000	7000	0.70	0.70	132.76	132.76
s3	63.5	63.9	7000	7000	0.70	0.70	132.76	132.76
s4	96.1	96.8	7000	7000	0.70	0.70	132.76	132.76
s5	190.0	190.0	7000	7000	0.70	0.70	132.76	132.76
s6	190.0	190.0	7000	7000	0.83	0.83	94.63	94.33
s7	80.2	80.3	470	470	0.83	0.83	94.63	94.33
s8	73.9	73.9	470	470	0.70	0.70	132.76	132.76
s9	58.1	58.1	470	470	0.70	0.70	132.76	132.76
s10	32.0	32.0	470	470	0.70	0.70	132.76	132.76
s11	190.0	190.0	7000	7000	0.37	0.37	38.13	38.43
s12	73.9	73.9	7000	7000	0.37	0.37	38.13	38.43
s13	61.4	61.3	470	470	0.37	0.37	38.13	38.43

3.3 Objective functions

Objective functions, decision variables and constraints are basic elements of an optimization problem [25]. In this research, thermal efficiency, annualized total cost and EI99 are used for energetic, economic and environmental (3E) performance evaluation, respectively.

3.3.1 Thermal efficiency

Mathematical model of the integrated system is established to quantify the thermal performance of this system. Energy balance equations for each equipment are listed in Table 5. The subscripts A refer to the absorption refrigeration cycle and the subscripts K refer to the Kalina cycle. m is the mass flow rate; h is the specific enthalpy; Q is heat flow; W is the electrical power consumption or electricity production; η_p and η_t are the overall efficiency of pumps and the turbine. Thermal efficiency of the generation cycle is adopted as the energetic objective in the multi-objective optimization model. The thermal efficiency η is defined as the ratio of net electricity output to the waste heat utilized in the generation cycle Q:

$$\eta=\frac{W_{\text{turbine}}-W_{\text{pump 1}}-W_{\text{pump 2}}}{Q} \quad (1)$$

Table 5 Energy balance equations for each equipment.

Equipment	Energy balance equation
Generator 1	$m_{A1}h_{A1}+Q_L=m_{A2}h_{A2}+m_{A6}h_{A6}$
Condenser	$Q_{condenser}=m_{A2}h_{A2}-m_{A3}h_{A3}$
Valve 1	$m_{A3}h_{A3}=m_{A4}h_{A4}$
Evaporator	$\|m_{A4}h_{A4}-m_{A5}h_{A5}\|=\|m_{K11}h_{K11}-m_{K1}h_{K1}\|$
Absorber	$m_{A5}h_{A5}+m_{A8}h_{A8}=m_{A9}h_{A9}$
Heat exchanger	$m_{A6}h_{A6}-m_{A7}h_{A7}=m_{A1}h_{A1}-m_{A10}h_{A10}$
Valve 2	$m_{A7}h_{A7}=m_{A8}h_{A8}$
Pump 1	$W_{pump\ 1}=\frac{1}{\eta_p}m_{A9}(h_{A10}-h_{A9})$
Generator 2	$m_{K4}h_{K4}+Q_H=m_{K5}h_{K5}+m_{K7}h_{K7}$
Turbine	$W_{turbine}=m_{K5}(h_{K5}-h_{K6})\times\eta_t$
Mixer	$m_{K6}h_{K6}+m_{K9}h_{K9}=m_{K10}h_{K10}$
High-temperature recuperator	$m_{K7}h_{K7}-m_{K8}h_{K8}=m_{K4}h_{K4}-m_{K3}h_{K3}$
Valve 3	$m_{K8}h_{K8}=m_{K9}h_{K9}$
Low-temperature recuperator	$m_{K10}h_{K10}-m_{K11}h_{K11}=m_{K3}h_{K3}-m_{K2}h_{K2}$
Pump 2	$W_{pump\ 2}=\frac{1}{\eta_p}m_{K1}(h_{K2}-h_{K1})$

3.3.2 Annualized total cost

Annualized total cost is selected as the economic indicator of the cascade waste heat recovery process. The annualized total cost calculation is conducted according to the procedure described in the book of Robin Smith [45]:

$$C_E=C_B\left(\frac{Q}{Q_B}\right)^M\frac{CEPCI_{2018}}{CEPCI_{2000}} \quad (2)$$

where Q is the equipment size; C_E is the cost for the equipment; Q_B refers to the base size of this equipment; C_B refers to the base cost; M is the cost exponent index according to the equipment type; $CEPCI_{2018}$ (603.1) and $CEPCI_{2000}$ (394.1) are Chemical Engineering Plant Cost Index employed in this work to keep the purchase price up to date [46].

$$C_F=[f_M f_P f_T(1+f_{pip})]C_E+(f_{er}+f_{inst}+f_{elec}+f_{util}+f_{os}+f_{build}+f_{sp}+f_{dec}+f_{cont}+f_{ws})C_E \quad (3)$$

where f_M, f_P and f_T are correction factors for construction material, design pressure and design temperature; f_{pip}, f_{er}, f_{inst}, f_{elec}, f_{util}, f_{os}, f_{build}, f_{sp}, f_{dec}, f_{cont} and f_{ws} are correction factors for pipe connection, equipment erection, instrumentation and controls, electrical, utilities, off-sites, buildings, site preparation, design engineering and construction,

contingency and working capital, respectively; C_F is the fixed cost for the whole system. Detailed equipment cost information and all the adopted correction factors are presented in Table 6 and Table 7.

Table 6 Equipment cost information and correction factors.

Equipment	Type	Unit	Q_B	$C_B \times 10^4$ \$	M	f_M	f_P	f_T
Generator 1	Storage tank	m^3	5	1.15	0.53	2.4	1.3	1.0
	Shell/tube heat exchanger	m^2	80	3.28	0.68	2.9	1.3	1.0
Condenser	Shell/tube heat exchanger	m^2	80	3.28	0.68	1.0	1.3	1.0
Evaporator	Shell/tube heat exchanger	m^2	80	3.28	0.68	2.9	2.0	1.0
Absorber	Storage tank	m^3	5	1.15	0.53	2.4	2.0	1.0
Heat exchanger	Shell/tube heat exchanger	m^2	80	3.28	0.68	2.9	1.3	1.0
Pump 1	Centrifugal pump	kW	1	0.20	0.35	3.4	2.0	1.0
Generator 2	Distillation column	t	8	6.56	0.89	2.1	1.5	1.0
	Sieve trays	m	0.5	0.66	0.91	2.4	1.5	1.0
Turbine	Compressor	kW	250	9.84	0.46	2.4	1.5	1.0
Mixer	Storage tank	m^3	5	1.15	0.53	2.4	1.0	1.0
HTR	Shell/tube heat exchanger	m^2	80	3.28	0.68	2.9	1.5	1.0
LTR	Shell/tube heat exchanger	m^2	80	3.28	0.68	2.9	1.5	1.0
Pump 2	Centrifugal pump	kW	4	0.98	0.55	2.4	1.5	1.0

Table 7 Correction factors.

Item	Value
Purchase price factor	1.0
f_{pip}	0.7
f_{er}	0.4
f_{inst}	0.2
f_{elec}	0.1
f_{util}	0.5
f_{os}	0.2
f_{build}	0.2
f_{sp}	0.1
f_{dec}	1.0
f_{cont}	0.4
f_{ws}	0.7

Finally, annualized total cost can be given as:

$$\mathrm{ATC} = C_F \frac{i(1+i)^n}{(1+i)^n - 1} \tag{4}$$

where i refers to the interest rate of 5%; n is the operation years of 15 years.

3.3.3 Eco-indicator 99 based on life cycle assessment

Life cycle assessment is an effective and comprehensive environment management tool for assessing environmental impacts of components, products or even

processes. Generally, there are four steps of LCA [31, 32]:

(1) Set goal and define scope. The aim of this study is to conduct LCA of a $LiBr/H_2O$ absorption chiller/Kalina cycle integrated system. Then, the environmental impacts based on LCA are employed as the environmental performance criteria in the proposed multi-objective optimization model of the integrated system. This integrated system has a design life span of 15 years. LCA of this system contains four stages: the construction phase, the transportation phase, the usage phase and the demolition phase. Environmental impacts during the extraction of raw materials and the production process are considered at the first stage. For the transportation stage, all these components are conventional equipment that can be obtained from suppliers within a distance of 200 km. In the usage phase, electrical power consumption of pumps is the major input for system operation. When the system reaches its service life, each part of the system is demolished differently. Metal materials are recycled, plastics are disposed by incineration and the remaining inert wastes are buried at waste landfill. Fig. 3 depicts the LCA boundary of the integrated system.

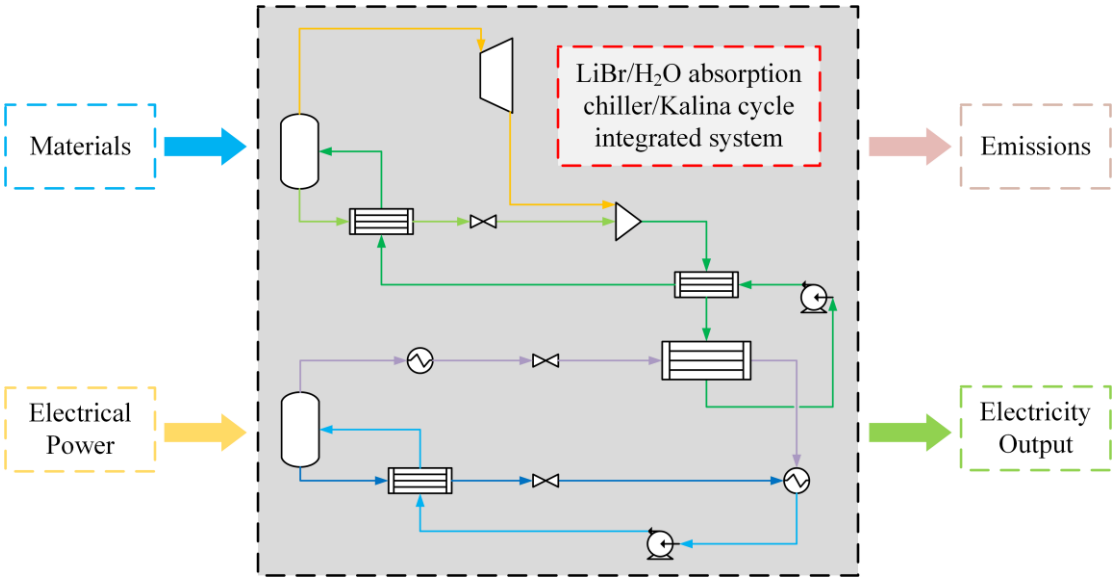

Fig. 3 LCA boundary of the integrated system.

(2) List life cycle inventory. This step considers and quantifies the input for system operation such as energy and resources, and the output of the system such as electrical work and emissions. The sizes of equipment, e.g. heat transfer area of heat exchangers, volume of storage tanks, mass of distillation column, etc., are obtained in the process simulation using Aspen Plus software. Construction materials information of all the components is carefully collected from suppliers and published works. Several construction materials with tiny usage amount are overlooked for modelling simplicity. Relevant materials and energy input are listed in Table 8. Diesel is consumed by trucks in the transportation phase. Electricity is purchased from local power grid for maintaining the continuous system operation. The rest LCA information is selected from GaBi database (Professional database 2018). Because the leakage of $LiBr/H_2O$ solution and ammonia solution is neglected, these chemicals constantly circulate in the system. Hence, the environmental impacts of working medium are not considered.

Table 8 Life cycle inventory of the absorption chiller/Kalina cycle integrated system.

Materials and energy input	Basic flows in Gabi process	Unit
Stainless steel (316)	Stainless steel cold rolled coil (316) [Metals]	kg
Carbon steel	Steel hot rolled coil [Metals]	kg
Cast iron	Cast iron [Metals]	kg
Rubber	Styrene-butadiene-rubber (SBR) [Plastics]	kg
Aluminum alloy	Aluminum sheet [Metals]	kg
Copper	Copper [Metals]	kg
Plastic	Polypropylene part (PP) [Plastic parts]	kg
Ceramic	Silicon Carbide [Minerals]	kg
Diesel	Diesel [Refinery products]	kg
Electricity	Electricity [Electric power]	kWh

(3) Life cycle impact assessment. According to the Eco-indicator 99 methodology [47], the life cycle impacts are generally divided as Human health damage, Ecosystem quality damage and Damage to resources. Human health indicators including Carcinogenic effects, Respiratory effects by organic substances, Respiratory effects by inorganic substances, Climate change, Ionizing radiation and Ozone layer depletion are

aggregated as Human health damage. The unit of this damage is Disability-Adjusted Life Years (DALY). It compares time lived with disability and time lost due to premature mortality [47]. Each lost life year before the normal life expectancy of each individual indicates a DALY value of 1. Ecosystem indexes are Ecotoxicity, Acidification/nutrification and Land use. Ecosystem quality damage is measured using the concept of potentially disappear fraction of species (PDF) from a specific area (m^2) over a period of time (year) as PDF·m^2·year. Resource depletion indicators are Minerals extraction and Fossil fuels extraction. Damage to resources means that extracting the same resources consumes more energy due to previous extraction of this type of resources, which is valued in terms of MJ of surplus energy. All these indicators are translated into a single index at the end using the weighting factors from the hierarchist perspective.

(4) Interpretation. All the obtained results are then fully interpreted from various aspects. In this multi-objective optimization problem, those points where substantial improvement of one objective can be obtained at an insignificant cost of other objectives should receive attention.

According to the principles of LCA, the environmental effects of this waste heat cascade utilization process are assessed. GaBi software version 8.0 is used to conduct the LCA modeling of the proposed system. Industrial ISO 14040 standard (2006) are followed. Eco-indicator 99 of eleven environmental impacts are currently employed to evaluate the end-point environmental effects of this integrated system. Based on the life cycle inventory, eleven environmental impacts are calculated at first [31, 48]:

$$IMP_{\mathrm{r}}=\sum_{\mathrm{b}} dm_{\mathrm{br}}\, LCI_{\mathrm{b}} \tag{5}$$

where IMP_{r} refers to the overall damage of impact category r, i.e. the total damage value of each environmental impact; LCI_{b} refers to the life cycle inventory associated with

chemical b, i.e. the amount of one certain substance; dm_{br} is the damage coefficient of chemical b in the impact category r, i.e. the effect of this substance on each environmental impact. The obtained environmental impacts are divided into three categories, i.e. Damage to Human health, Damage to Ecosystem quality and Damage to resources. Hence, the overall damage of each damage category can be obtained by summing up all the environmental impacts in this category:

$$DAM_d = \sum_r IMP_r \quad (6)$$

where DAM_d is the overall damage value of damage category d. These end-point indicators have to be normalized and weighted before to be aggregated into a single index EI99. The normalization and weighting factors from the hierarchist perspective with average weighting are commonly used [47]. Finally, the three damage categories are combined as a single evaluation index:

$$EI99 = \sum_d n_d w_d DAM_d \quad (7)$$

where and n_d and w_d are normalization factors and weighting factors for damage category d. EI99 is hence employed as the major criterion of the environmental performance in the proposed multi-objective optimization model.

3.4 Decision variables and constraints

Concentrations of $LiBr/H_2O$ solution and NH_3/H_2O basic solution are fixed to eliminate the flow uncertainty and to simplified the optimization model. Thus, the main decision variables are refrigeration temperature of the absorption chiller, basic solution temperature at the outlet of evaporator, the turbine outlet pressure (backpressure) and the segment temperature. Decision variables and constraints are listed in Table 9. In addition, some extra constraints are given as follow:

1. The given waste heat has to be completely recovered in the cascade process;
2. The cold-in/hot-out temperature difference in the evaporator is higher than 5 °C (i.e.

$T_{evap\text{-}hot\text{-}outlet}$ - $T_{refrigeration} \geq 5$ °C);

3. When the outlet temperature at the evaporator hot side is 7 °C, the turbine outlet pressure should be higher than 293 kPa to avoid ammonia vapor releasing from the basic solution in the pump. This backpressure should also be lower than the inlet pressure which is fixed at 3300 kPa.

4. Cooling capacity of the absorption chiller has to meet the demand in Kalina cycle.

Table 9 Decision variables and constraints.

Decision variables	Unit	Constraints
Refrigeration temperature (stream A4)	°C	$2 < T_{refrigeration} < 10$
Evaporator hot side outlet temperature (stream K1)	°C	$7 < T_{evap\text{-}hot\text{-}outlet}$
Turbine backpressure (stream K6)	kPa	$293 < P_{back} < 3300$
Segment temperature	°C	$119.4 < T_{segment} < 119.5$

3.5 Non-dominated sorting genetic algorithm II

Compared with single objective optimization, multi-objective optimization is to produce a set of optimization results, the Pareto optimal solutions. It is impossible to obtain one solution which achieves all the optimal objectives because these objectives always contradict with each other [49]. The decision makers can select the preferred solution from these Pareto frontiers according to the actual needs. Non-dominated sorting genetic algorithm II (NSGA-II) is seen as a fast genetic algorithm for solving multi-objective optimization problem. It has strengths such as fast non-dominated sorting process, elitist strategy and less parameters [49]. Detailed parameter settings are presented in Table 10. As shown in Fig. 4, the multi-objective optimization using NSGA-II technique has following steps [21, 25, 32, 33]:

Step 1: Random initialization of population: the generated population is of size N within the lower and upper limits;

Step 2: Fitness evaluation of each individual: each individual will be given a fitness scores of objective functions;

Step 3: Parent population selection according to non-dominant sorting and crowding distance sorting: front values are assigned for each individual according to its non-domination in the population, a crowding distance is also determined for those individuals in the same front according to the closeness with others, then the whole population is sorted and those with lesser rank value and larger crowding distance are selected as paternal population using tournament selection;

Step 4: Crossover and Mutation: offspring population is generated from the selected parent population through crossover and mutation, simulated binary crossover for the retention of elite individuals and polynomial mutation for the diversity of population are hence performed;

Step 5: Combination of parent population and offspring population: a combined population of size 2N is thus formed, it is then evaluated and sorted, only the best N individuals are selected for offspring generation to ensure the elitism, the procedures from Step 2 to Step 5 will be repeated until the termination criteria is satisfied or the max generation number is reached.

Table 10 Tuning parameters and settings for NSGA-II.

Parameters	Value
Decision variables	4
Objective functions	3
Population size	100
Number of generations	500
Initialization mode	Random
Selection process	Tournament
Tournament size	2
Crossover probability	0.9
Mutation probability	0.1
Crossover distribution index	20
Mutation distribution index	20

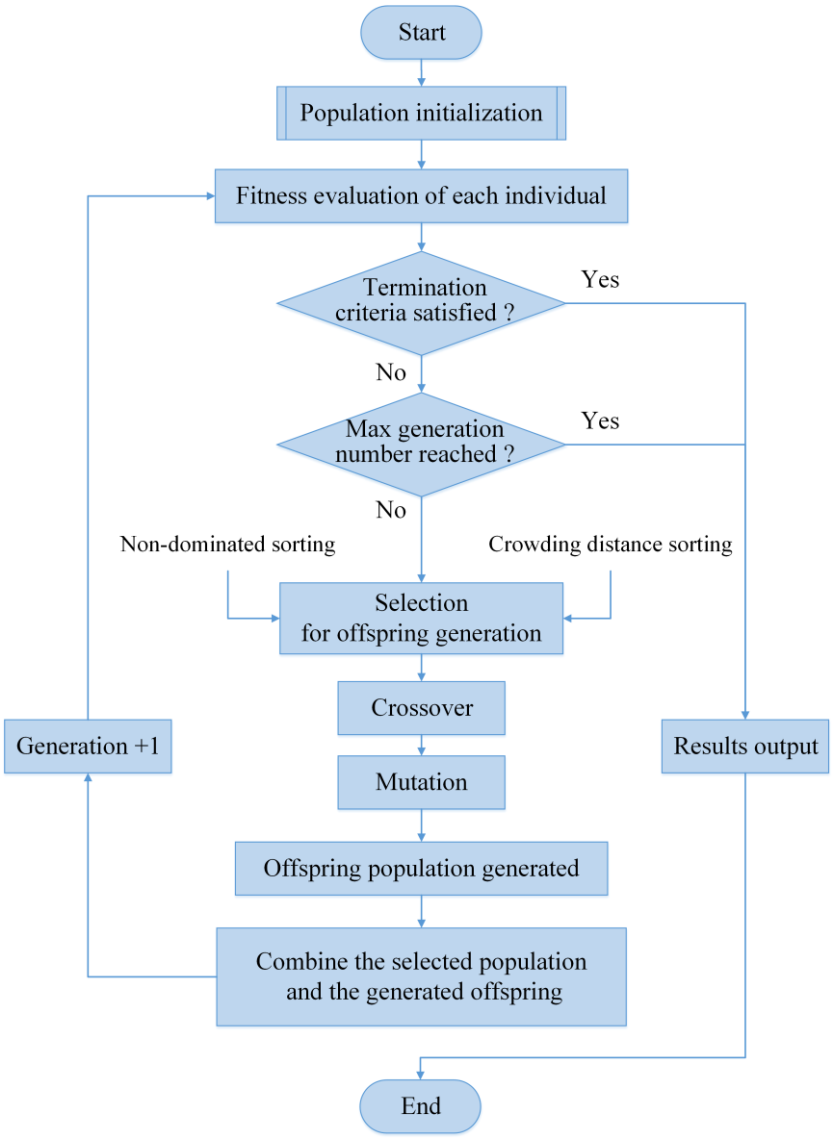

Fig. 4 Flowchart of NSGA-II for multi-objective optimization of the proposed system.

3.6 Decision-making method

Pareto optimal solutions obtained in this research represent the optimal trade-off among the energetic, economic and environmental performance of this integrated system. Post-optimal analysis encourages researchers to focus on the Pareto solutions where significant improvements can be achieved at an insignificant cost of another objective [31]. TOPSIS method and Shannon entropy approach was coupled as a novel decision-making method [50]. TOPSIS is an available decision-making method for

final optimal solution selection. The final optimal solution is selected with the shortest distance from the ideal point and the farthest distance from the non-ideal point [23, 24]. Shannon entropy approach can determine weights for different objectives such as thermal efficiency, ATC and EI99 in this research without considering the preference. TOPSIS method and Shannon entropy approach are hence employed for decision-making in this work.

4. Results and discussions

4.1 Pareto optimal solutions and optimization schemes

Thermal efficiency, annualized total cost and EI99 are selected as three objectives in the proposed multi-objective optimization model. NSGA-II, the elitism genetic algorithm, is employed for solving the optimization problem in this work. Based on the parameter specifications, process assumptions, decision variables and constraints mentioned above (in section 3), a series of Pareto optimal solutions has been obtained. As shown in Fig. 5, this Pareto solution set represents the alternative solutions for current optimization problem. It can be noticed that the Pareto solutions are basically plotted as a continuous line, especially when the population size in the genetic algorithm is large enough. With the variation of decision variables, these three objectives vary within certain ranges. Thermal efficiency changes in the range from 15.31% to 16.78%. ATC has a minimum value of 1.79×10^5 \$ and a maximum value of 1.85×10^5 \$. The variation range of the environmental index EI99 is from -6.52×10^5 to -7.17×10^5. The integrated system is a cascade waste heat recovery system and it utilizes waste heat to produce electrical power, reducing emissions as a result. Therefore, the values of EI99 are obtained as negative values in current research.

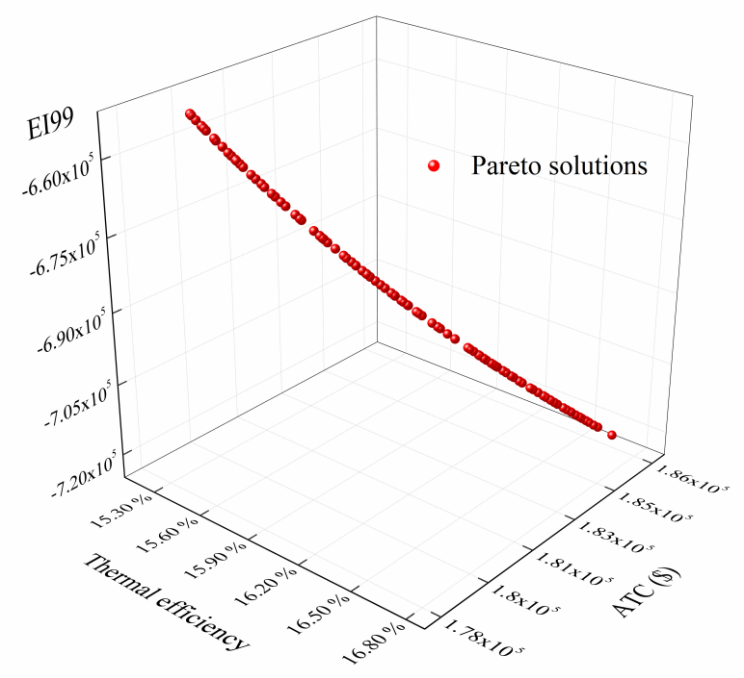

524

525 **Fig. 5** Pareto optimal solutions of the proposed multi-objective optimization model.

526

527 Fig. 6 presents the relationship between each two objectives: thermal
528 efficiency/ATC, ATC/EI99 and thermal efficiency/EI99, to give a clearer illustration of
529 the trade-off among the energetic, economic and environmental performance. The
530 relationship between thermal efficiency and ATC can be seen as a non-linear positive
531 function. Higher economic cost is required for achieving a better energetic performance.
532 It is because better heat transfer always requires a lager heat transfer area, higher
533 electrical power production requires a more powerful turbine, etc. Larger sizes of
534 equipment will result in higher purchase prices. It can also be noticed that with further
535 improvement on the energetic performance, the ATC increases more rapidly and hence
536 the economic performance could be rather poor. In the second figure, with the increase
537 of ATC, the environmental performance becomes better while this trend slows down
538 gradually. There is an obvious conflict between these two indicators. Also, the
539 relationship between ATC and EI99 is nonlinear. However, thermal efficiency has a
540 nearly linear relationship with the environmental index EI99. More electrical power

production can be achieved in the integrated system with higher thermal efficiency. This also leads to a more significant reduction of emissions, from an environmental point of view. Hence, it can be arbitrarily concluded that this linear relationship is caused by the actual electricity production from the integrated system. Decision makers can choose any of the Pareto solutions according to his/her own preference. It indicates that each point of this solution set can be seen as one reasonable solution to current optimization problem. In this work, TOPSIS method and Shannon entropy approach are combined and then used for the decision-making process without any personal preference. This final optimal solution is selected from the Pareto optimal solutions as the multi-objective optimized scheme of the integrated system. In general, there are four operation schemes for this integrated system: scheme aiming at optimal thermal efficiency (Scheme 1), scheme aiming at optimal ATC (Scheme 2), scheme aiming at optimal EI99 (Scheme 3) and the multi-objective optimized scheme (Scheme 4).

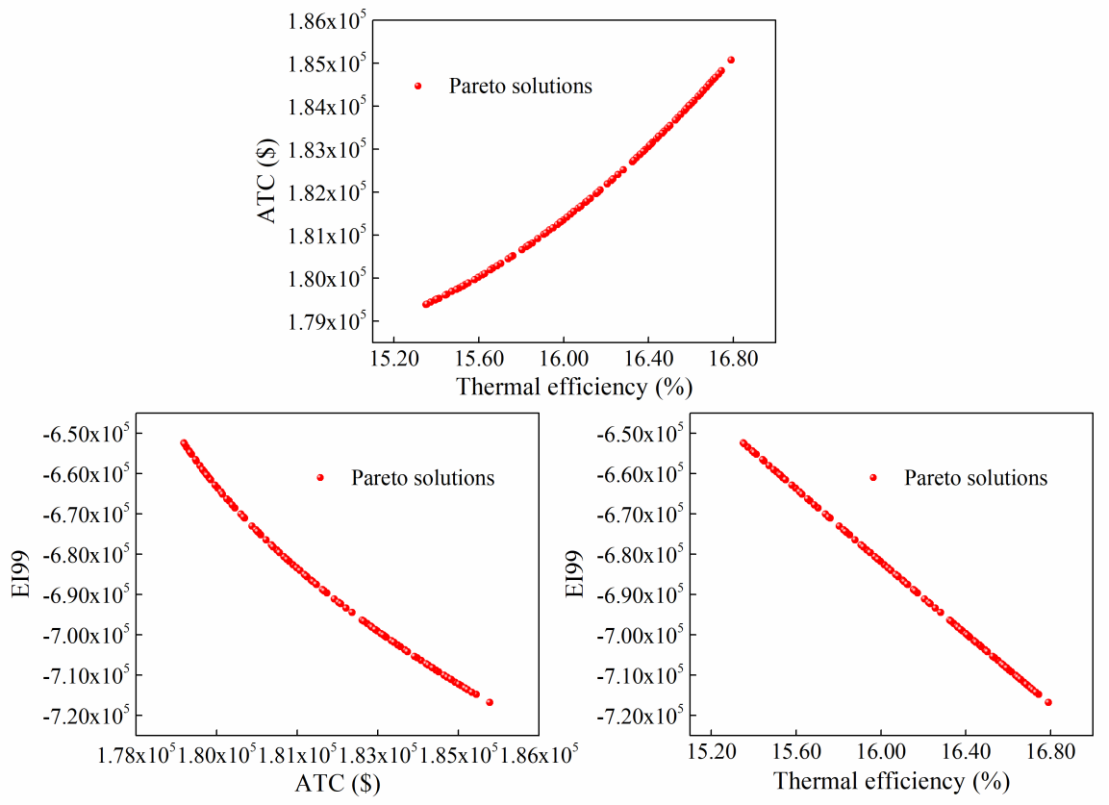

Fig. 6 Relationship between each two objectives.

All the optimization schemes and relevant operation parameters are presented in Table 11. Lower refrigeration temperature would be beneficial to energetic and environmental performance except for the economic indicator. When the refrigeration temperature is lower, the hot side outlet temperature of the evaporator could be also lower. Hence lower backpressure of KC can be reached, resulting in a higher turbine expansion ratio and more electrical power generation. More electricity production means less consumption of fossil fuels and more emissions reduction. Segment temperature, the temperature dividing the low-grade waste heat into two parts, shows no significant variation for all the operation schemes. Scheme 1 and Scheme 3 have exactly the same operation parameters, indicating that the optimal energetic performance and optimal environmental performance can be achieved simultaneously. Scheme 2 has the best economic performance while the other two indicators are the worst. The multi-objective optimized scheme (Scheme 4) presents around 9.34% and 9.53% higher than the minimum thermal efficiency and EI99 at the cost of 3.03% higher ATC. Therefore, with sufficient consideration of three different objectives, this final optimal solution is superior to other solutions.

Table 11 Optimization schemes and operation parameters.

Scheme No.	η	ATC ($)	EI99	$T_{refrigeration}$	$T_{evap\text{-}hot\text{-}outlet}$	P_{back}	$T_{segment}$
1	16.78%	1.85×10^5	-7.17×10^5	2 °C	7 °C	293 kPa	119.5 °C
2	15.31%	1.79×10^5	-6.52×10^5	10 °C	15 °C	395 kPa	119.4 °C
3	16.78%	1.85×10^5	-7.17×10^5	2 °C	7 °C	293 kPa	119.5 °C
4	16.74%	1.85×10^5	-7.15×10^5	2.26 °C	7.25 °C	296 kPa	119.5 °C

4.2 Life cycle assessment of the cascade waste heat recovery system

Life cycle assessment is comprehensively conducted for the proposed system. Eco-indicator 99 method is adopted to investigate the end-point environmental effects. Eleven life cycle impacts are: Carcinogenic effects, Respiratory effects by organic

substances, Respiratory effects by inorganic substances, Climate change, Ionizing radiation and Ozone layer depletion of Human health damage category; Ecotoxicity, Acidification/nutrification and Land use of Ecosystem damage category; Minerals extraction and Fossil fuels extraction of Resource damage category. These impacts are aggregated into the overall environmental index EI99 using normalization and weighting factors. Environmental impacts, damage categories and EI99 at the four stages are listed in Table 12. Both resources consumption and various emissions will increase the value of a certain impact. However, the absorption chiller/KC integrated system is a waste heat recovery system which recovers waste heat to produce electrical power, reducing relevant consumptions and emissions as a result. Therefore, many environmental impacts have negative values. Carcinogenic effects are mainly at the usage stage of this system, influenced by reducing emissions to air (66%), fresh water (16%) and agricultural soil (18%). These emissions are basically composed of heavy metals such as arsenic (56%) and cadmium (44%). Impact of Climate change is greatly influenced by inorganic emissions (basically carbon dioxide) to air (94%) and organic emissions (methane) to air (5%). Ionizing radiation is influenced by reducing radioactive emissions of C14 (92%). Respiratory effects caused by inorganic substances are inorganic emissions of nitrogen oxide (22%) and sulphur oxide (17%), particles to air such as dust PM 2.5 (14%), PM 2.5~10 (20%) and PM10 (27%). Respiratory effects (Organic) in this work refer to organic emissions including xylene (52%), alkene (12%), ethyl benzene (9%), etc. Ecotoxicity results from heavy metals pollution such as nickel (38%), lead (19%), zinc (26%), chromium (13%), etc., in the use of electricity. Acidification and nutrification are mainly determine by reducing nitrogen oxide (81%) and sulphur oxide (18%) emissions. Fossil fuels extraction is related to the usage of non-renewable energy resources of hard coal (64%), crude oil (9%), natural gas (17%),

etc. Land use is regarded as a damage because the occupied area cannot be restored to the natural status. This impact is not considered in this research because the sizes of both the devices and the whole system are not extremely large. Generally, all the environmental impacts are significantly influenced by the electricity generation in the usage phase, except for the Ozone layer depletion and Minerals extraction. The former impact has the highest value at the construction stage caused by the halogenated organic emissions such as R11 (46%) and R114 (40%) during the stainless steel manufacturing process. The latter one is mainly at the construction stage also for stainless steel production because of the consumptions of non-renewable elements such as molybdenum (37%) and nickel (56%). It is also influenced by the copper production process. All these impacts are then normalized and assigned into corresponding damage categories. In the construction phase, Damage to resources is remarkable compared with other two categories. It indicates a significant resource degradation for the production of construction materials. In the transportation phase, Damage to ecosystem seems to be less significant than the other categories. At the third stage of the life cycle, almost all the impacts have negative values because of the considerable electrical power generation. The relevant resources and energy consumptions are hence reduced. During this period, Human health damage occupies the largest proportion, which suggests that it is more beneficial to human health using waste heat to generate electricity. When the system reaches its service life, metal materials are recycled, plastics are disposed by incineration and the inert wastes are buried at waste landfill. It can be found that the demolition of the whole system will do harm to human health and ecosystem (except for impact of Ecotoxicity) while it is good for the Minerals extraction.

628 **Table 12** Environmental impacts, damage categories and EI99 of Eco-indicator 99 method at each stage.

Environmental impact	Unit	Construction	Transportation	Usage	Demolition	Total
Carcinogenic effects	DALY	4.56×10^{-3}	1.78×10^{-5}	-0.15	8.24×10^{-6}	-0.15
Climate change	DALY	5.33×10^{-3}	2.57×10^{-5}	-1.26	7.78×10^{-4}	-1.25
Ozone layer depletion	DALY	1.27×10^{-6}	2.67×10^{-15}	-1.69×10^{-9}	4.84×10^{-8}	1.32×10^{-6}
Ionizing radiation	DALY	6.35×10^{-6}	6.73×10^{-10}	-8.42×10^{-4}	3.23×10^{-6}	-8.32×10^{-4}
Respiratory effects (Inorganic)	DALY	2.36×10^{-2}	4.68×10^{-5}	-5.08	7.55×10^{-4}	-5.05
Respiratory effects (Organic)	DALY	8.68×10^{-6}	2.17×10^{-8}	-2.72×10^{-3}	8.04×10^{-7}	-2.71×10^{-3}
Ecotoxicity	PDF·m^2·yr	3.20×10^{3}	0.29	-2.91×10^{5}	-2.03	-2.87×10^{5}
Acidification/nutrification	PDF·m^2·yr	6.33×10^{2}	2.57	-9.01×10^{4}	26.42	-8.94×10^{4}
Land use	PDF·m^2·yr	0.00	0.00	0.00	0.00	0.00
Minerals extraction	MJ surplus energy	1.44×10^{4}	1.07×10^{-2}	-5.18×10^{3}	-2.83×10^{2}	8.97×10^{3}
Fossil fuels extraction	MJ surplus energy	2.54×10^{4}	1.90×10^{2}	-1.39×10^{6}	7.82×10^{3}	-1.36×10^{6}
Damage category	Weighted factor	Construction	Transportation	Usage	Demolition	Total
Human health	400	7.09	2.44×10^{-2}	-1.15×10^{3}	0.53	-1.14×10^{3}
Ecosystem	400	5.63	7.21×10^{-3}	-5.98×10^{2}	0.07	-5.93×10^{2}
Resources	200	1.01×10^{2}	2.30×10^{-2}	-2.04×10^{2}	-0.97	-1.04×10^{2}
EI99		2.52×10^{4}	17.23	-7.40×10^{5}	46.69	-7.14×10^{5}

629

630

631 Different construction materials impose different effects on the environmental
632 impacts at the construction stage as well as the demolition stage. Contributions of each
633 materials to ten environmental impacts (impact of Land use is excluded) at the first
634 stage are depicted in Fig. 7. All the environmental impacts have positive values hence
635 the manufacturing process makes all these indicators worse. The working media in this
636 proposed system are corrosive fluids of LiBr/H_2O solution and ammonia solution. For
637 this reason, stainless steel is the major construction material for all devices except for
638 the condenser of the absorption chiller. Carbon steel is selected for this condenser
639 because the fluids in it are pure water. Hence, stainless steel production occupies the
640 largest proportion of all the environmental impacts. Cast iron production has an obvious
641 effect on the Ionizing radiation impact because of radioactive emissions to air. Except
642 for this, rubber manufacturing has certain influences on the Fossil fuels extraction,
643 Respiratory effects (Organic) and Ionizing radiation. Carbon steel production causes
644 the second large effect on the Climate change due to carbon dioxide emissions.
645 Aluminum alloy manufacturing imposes the second large effect on the impact of Ozone
646 layer depletion. The effects on environmental indicators of ceramic, plastic and copper
647 production are basically insignificant due to the relatively small amount of these
648 materials.

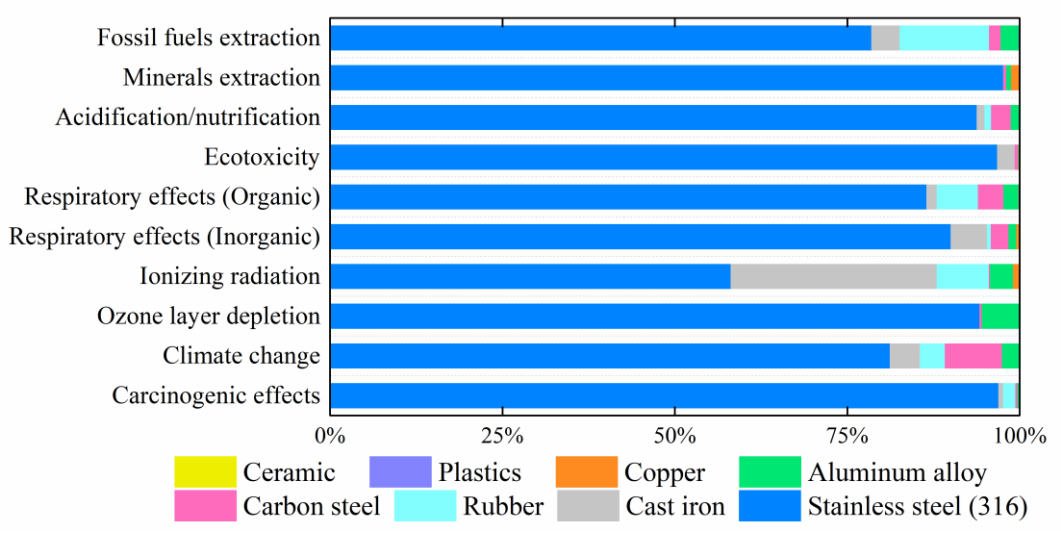

Fig. 7 Contributions of each materials at the construction stage.

Fig. 8 presents the environmental impacts of these materials in the demolition phase. Plastics are disposed by incineration and other inert wastes are buried. Only metal materials are recycled at the demolition stage. It is very obvious that recycling copper has a totally different effect on these indicators. Minerals extraction, Ecotoxicity and Carcinogenic effects have considerable negative values during this recycling process. Recycling copper presents totally different situation because the copper production has a complex process and causes more damage to the environment due to heavy metals pollution to air, fresh water and agricultural soil. It indicates that copper recycling is beneficial to these environmental aspects, especially alleviating the heavy metals pollution and reducing the copper mining consumption. The heavy metals pollution will pose a serious threat to human health and the whole ecosystem. Therefore, copper recycling should be taken seriously. For the positive values (caused damage) at this last stage, stainless steel recycling also imposes the largest harm to the environment, followed by carbon steel and cast iron recycling. Disposing the rest construction materials has insignificant influence on these environmental indicators because of the little use of these materials.

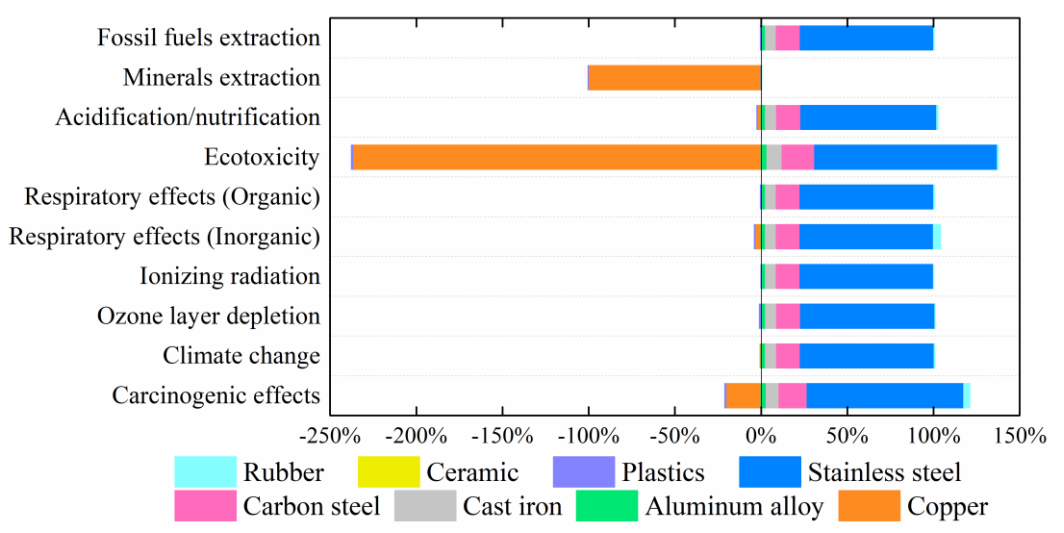

Fig. 8 Contributions of each materials at the demolition stage.

Two types of emissions are mainly considered in the transport phase: the direct emissions and indirect emissions. Direct emissions refer to emissions of the use of trains, cars, etc. Trucks complying to Euro 5 norm, with gross weight of 12-14 tons and payload capacity of 9 tons, are selected from the Gabi database. Indirect emissions are emissions of using the fossil fuels. Diesel from local filling station is used as the fuel in the transportation phase. Comparisons between direct/indirect emissions at this stage are depicted in Fig. 9. Carcinogenic effects, Ozone layer depletion, Ionizing radiation, Ecotoxicity, Minerals extraction and Fossil fuels extraction are exclusively caused by burning this fossil fuel. Diesel consumption also has more significant effect on the Respiratory effect (Organic). For environmental impacts of Climate change, Respiratory effects caused by inorganic substances and Acidification/nutrification, the use of trucks imposes the dominant effects comparing with the fuel usage.

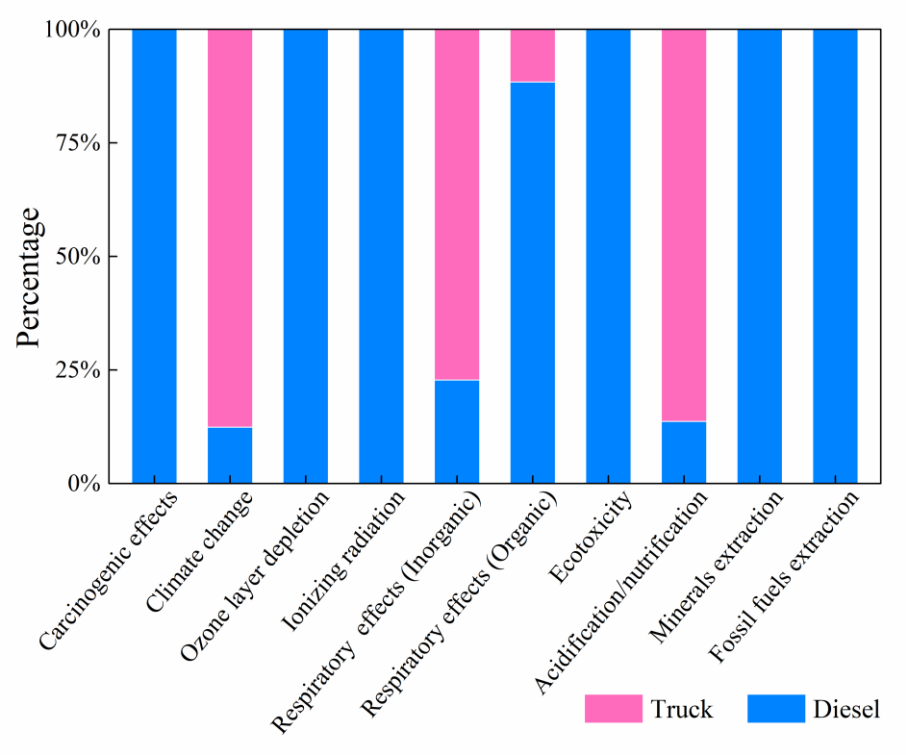

683

684 **Fig. 9** Comparison between direct/indirect emissions at the transportation stage.

685

686 From the life cycle assessment of the integrated system, it can be noticed that the
687 overall LCA environmental performance is greatly influenced by the electricity
688 production at the usage stage. Hence the effects of operational parameters on the
689 environmental performance should be investigated. Except for the decision variables,
690 i.e. refrigeration temperature, turbine outlet pressure, segment temperature, etc., there
691 are still many other operational parameters in this integrated system, such as solution
692 concentration, condenser temperature, absorber temperature, equipment efficiency, etc.
693 As the refrigeration temperature is the most critical operation parameters related to
694 electrical power production, effect of refrigeration temperature on these environmental
695 impacts should be investigated. The variations of eleven environmental impacts and
696 three damage categories for different refrigeration temperature are illustrated in Fig. 10.
697 In the Damage to Human health category, the curves at the upper position, i.e., Ozone
698 layer depletion, Ionizing radiation, Respiratory effects (Organic) and Carcinogenic

effects, have no obvious change with the increase of refrigeration temperature. However, impacts of Respiratory effects (Inorganic) and Climate change present observable variation with the increasing refrigeration temperature. In the Damage to Ecosystem quality category, Acidification/nutrification and Ecotoxicity impacts are influenced by the refrigeration temperature (Land use is not considered). In the Damage to Resources category, only the impact of Fossil fuels extraction shows observable variation. Five environmental impacts, i.e. Respiratory effects (Inorganic), Climate change, Acidification/nutrification, Ecotoxicity and Fossil fuels extraction present observable increase with the refrigeration temperature. These impacts are highly related to the emissions of carbon dioxide, nitrogen oxide, sulphur oxide and particulate matters or the use of non-renewable energy resources. These emissions to air or resources consumption can be reduced by realizing more electrical power production in the proposed system at lower refrigeration temperature. This explains the reason for the better environmental performance of this proposed system at lower refrigeration temperature. Emissions reduction due to the electrical power generation in this waste recovery system improves the environmental indicators of Climate change, Respiratory effects cause by Inorganic substances, Ecotoxicity, Acidification/nutrification and Fossil fuels extraction (descending order). For the three damage categories, Damage to Human health presents the most obvious upward trend with the increasing refrigeration temperature. Hence, electrical power generation using the waste heat would achieves substantial improvement on the human health.

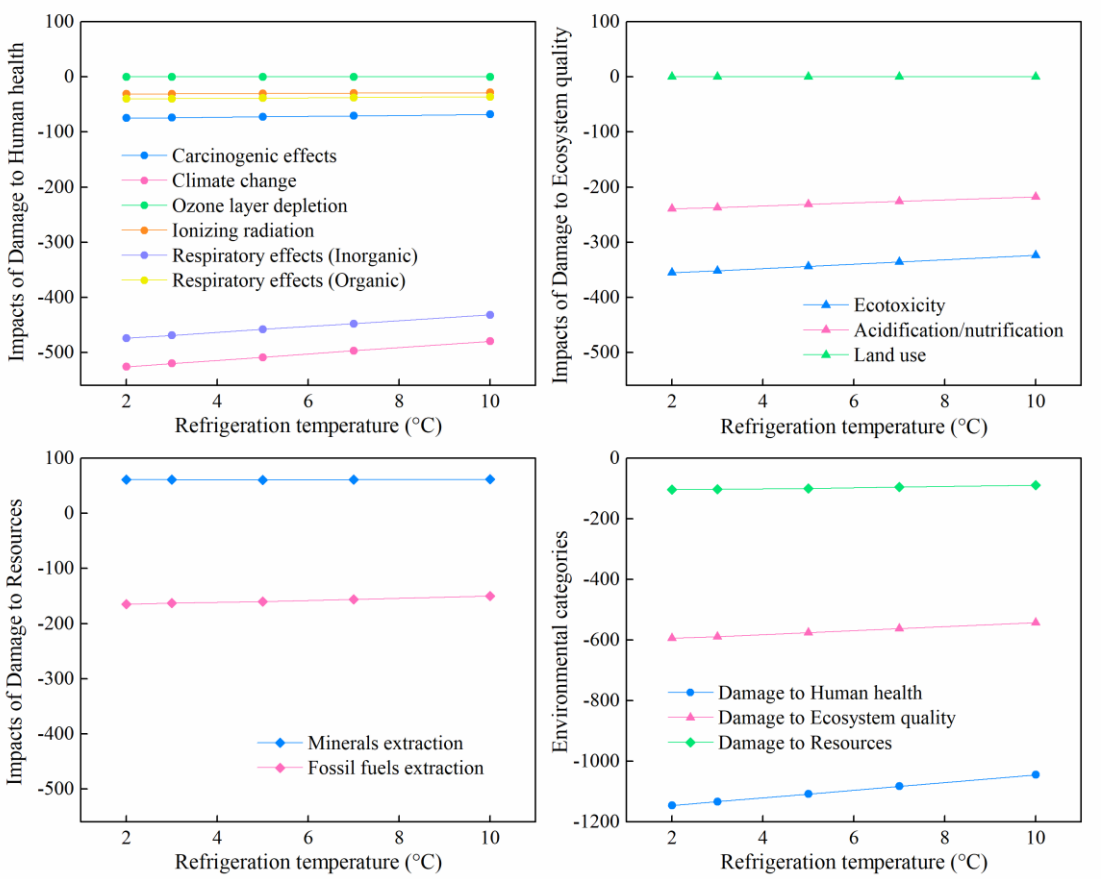

Fig. 10 Effect of refrigeration temperature on different environmental impacts and categories.

4.3 Life cycle assessment of the integrated system and individual Kalina cycle

LiBr/H_2O absorption refrigeration cycle in this work utilizes the waste heat from the Kalina cycle to provide cooling capacity. This absorption chiller is hence employed as an auxiliary cooling cycle for the KC to fully utilized the waste heat in cascade. It is very necessary to make comparisons between the integrated system and the individual Kalina cycle. In our previous research [34], the proposed system achieved more net electrical power generation than the individual KC. However, these two waste heat recovery systems have never been compared from the environmental aspect. In this section, the integrated system is compared with the individual KC using two life cycle impact assessment method: Eco-indicator 99 and CML 2001. Eco-indicator 99 method is used for end-point environmental comparisons and CML 2001 method is adopted for

mid-point environmental evaluation. Comparisons of environmental impacts, damage categories and the final index EI99 between the integrated system and the individual KC are given in Table 13. The improvement on these environmental indicators has also been calculated. Positive values refer to the environmental damage while negative values are environmental improvement due to emissions reduction. Comparison results show that except the Ozone layer depletion impact of the integrated system is slightly worse than that of the individual KC, the rest environmental indicators of the integrated system are generally better than those of the individual KC. After the integration, Damage to Human health, Damage to Ecosystem quality and Damage to resources are improved by 44.82%, 45.00% and 107.92%, respectively. The overall environmental index EI99 is improved by 46.17%. It suggests that compared with the individual KC, the integrated system has a better environmental performance.

Table 13 Eco-indicator 99 comparisons between the integrated system and individual KC.

Damage category	Environmental impact	Integrated system	Individual KC	Improvement
Human health	Carcinogenic effects	-74.54	-51.05	46.01%
	Climate change	-524.12	-362.20	44.70%
	Ozone layer depletion	6.01×10^{-3}	5.41×10^{-3}	11.09%
	Ionizing radiation	-31.06	-21.44	44.87%
	Respiratory effects (Inorganic)	-472.26	-326.23	44.76%
	Respiratory effects (Organic)	-39.66	-27.41	44.69%
	Total	-1141.63	-788.32	44.82%
Ecosystem	Ecotoxicity	-354.31	-244.21	45.08%
	Acidification/nutrification	-238.49	-164.62	44.87%
	Land use	0	0	/
	Total	-592.80	-408.83	45.00%
Resources	Minerals extraction	60.59	63.20	-4.13%
	Fossil fuels extraction	-164.53	-113.19	45.36%
	Total	-103.94	-49.99	107.92%
EI99		-7.14×10^{5}	-4.89×10^{5}	46.17%

In addition, CML 2001 is also regarded as an available life cycle impact assessment method which simulates the mechanism between the pollutants and the

caused damage from the mid-point perspective [51]. The CML 2001 method considers various impacts such as Global warming potential (GWP), Acidification potential (AP), Ozone layer depletion potential, etc. For waste heat recovery system as presented in this research, climate change is the first thing should be considered. Impacts of Global warming potential and Acidification potential are adopted as the mid-point evaluation indicators. Therefore, carbon footprints and Acidification potential of both systems are obtained and then compared from the mid-point perspective. GWP 100 years is used to evaluate carbon footprint by calculating the equivalent emissions of CO_2 and Acidification potential is measured utilizing the equivalent emissions of SO_2.

Comparisons between the proposed system and individual KC in terms of GWP 100 years are presented in Fig. 11. It can be noticed that the balance of equivalent CO_2 emissions of these two systems can be achieved in around 0.1 year. This means that the GWP caused in the construction and transportation phases can be eliminated with only a month or so. Except for the demolition stage, the curves of equivalent CO_2 emissions at the first three stages are basically linear variation. The fitted correlations during this period are obtained for both systems: $y_{GWP}=-4.06\times10^5x+2.57\times10^4$ for the integrated system and $y'_{GWP}=-2.81\times10^5x+2.11\times10^4$ for the individual KC (y_{GWP} and y'_{GWP} are GWP values on the ordinate and x is year on the abscissa). Then the intersection of two curves is calculated as around 0.04 year (around 14 days). This intersection indicates that the emissions reduction of equivalent CO_2 in the proposed system surpasses that in the individual KC within a very short period of time. The curves of both systems present little variation at the demolition stage, which indicates that the environmental effect at this stage is insignificant. When both systems reach to the service life, the integrated system shows a 44.70% higher performance than the individual KC. It means that the integrated system achieves much more emissions reduction than the individual KC.

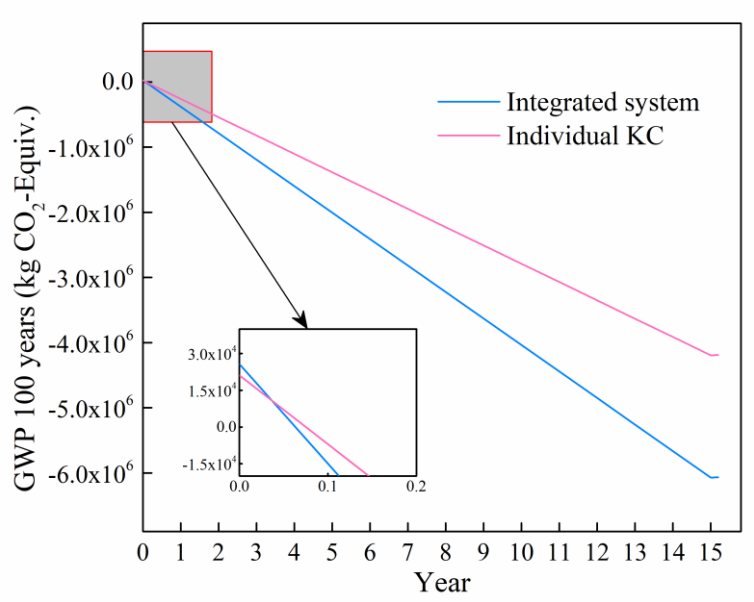

775

776 **Fig. 11** Global Warming Potential with time for the proposed system and individual KC.

777

778 Comparisons between two systems in terms of Acidification potential are
779 presented in Fig. 12. The equivalent SO_2 emissions balance of two systems is achieved
780 in around 0.2 year thus the Acidification potential from the construction and
781 transportation process is quickly eliminated. The fitted correlations of equivalent SO_2
782 emissions are also obtained: y_{AP}=-1.70×10^3x+308.50 for the integrated system and
783 y'_{AP}=-1.18×10^3x+277.69 for the individual KC (y_{AP} and y'_{AP} are AP values on the
784 ordinate). The intersection is calculated as around 0.06 year (around 21 days). This
785 intersection indicates that the equivalent SO_2 emissions reduction in the proposed
786 system will quickly surpass that in the individual KC. The variation of equivalent SO_2
787 emissions at the demolition stage is also insignificant. When the last stage is finished,
788 the integrated system reduces much more equivalent SO_2 emissions than the individual
789 KC, with the improvement of 45.12%.

790

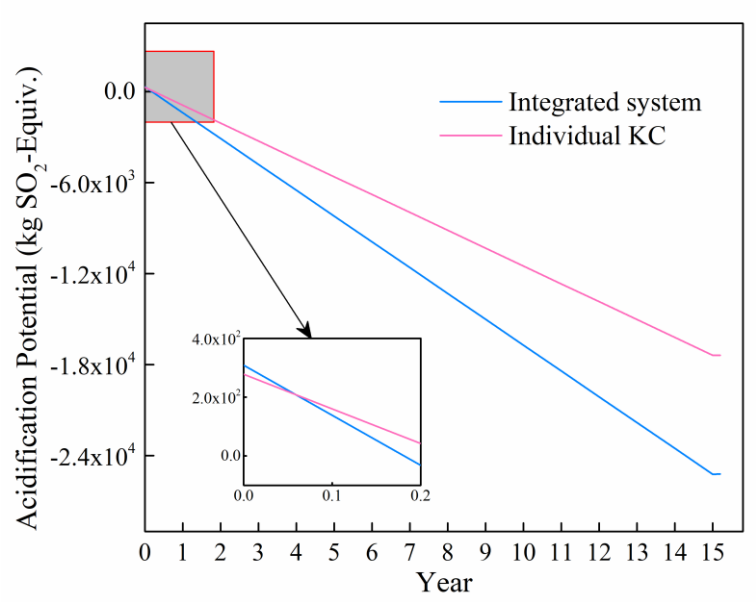

Fig. 12 Acidification Potential with time for the proposed system and individual KC.

In general, based on the mid-point and end-point comparisons of environmental indicators between these two systems, it can be concluded that this proposed system is a better than the individual KC from the environmental point of view.

5. Conclusions

Multi-objective optimization of an absorption chiller/KC integrated system is investigated from the energetic, economic and environmental aspects. LCA is inserted into the optimization model to evaluate the environmental performance. NSGA-II is employed to solve the conflicts among objectives. TOPSIS and Shannon entropy approach are combined for decision making. Pareto optimal solutions are obtained, presenting the optimal trade-off among objectives. LCA of the proposed system and the individual KC is comprehensively conducted and compared, using Eco-indicator 99 method and CML 2001 method. Main conclusions are as follows:

(1) The final optimal solution presents around 9.34% and 9.53% higher thermal efficiency and EI99 at the cost of 3.03% higher ATC.

(2) Environmental damages are mainly caused in the construction, transportation and demolition phases. But the electricity production at the usage stage determines the final LCA environmental results.

(3) Manufacturing and recycling of stainless steel have dominant environmental effects. Copper recycling has considerable contributions to the environmental performance improvement.

(4) Low refrigeration temperature is beneficial to energetic and environmental performance, but not for the economic performance. More electricity production at lower refrigeration temperature improves the environmental indicators.

(5) Mid-point analysis of carbon footprints and Acidification potential indicates that the equivalent CO_2 and equivalent SO_2 emissions balance can be achieved in around 0.1 year and 0.2 year, respectively.

(6) From the end-point and mid-point aspects, comparison results prove that this integrated system is obviously better than the individual Kalina cycle.

Declarations of interest: none

Acknowledgements

Funding: This work was supported by the National Natural Science Foundation of China [grant number 51676209]; the Foundation of Key Laboratory of Low-Carbon Conversion Science & Engineering, Shanghai Advanced Research Institute, Chinese Academy of Sciences [grant number KLLCCSE-201907]; the Fundamental Research Funds for the Central Universities of Central South University [grant number 2017zzts129].

834 **Reference**

835 [1] Zhang X, He M, Zhang Y. A review of research on the Kalina cycle. Renew Sust
836 Energ Rev 2012;16(7):5309-18.
837 [2] Coskun A, Bolatturk A, Kanoglu M. Thermodynamic and economic analysis and
838 optimization of power cycles for a medium temperature geothermal resource. Energ
839 Convers Manage 2014;78:39-49.
840 [3] Ma W, Xue X, Liu G. Techno-economic evaluation for hybrid renewable energy
841 system: Application and merits. Energy 2018;159:385-409.
842 [4] Rashidi J, Yoo C. Exergy, exergo-economic, and exergy-pinch analyses (EXPA) of
843 the kalina power-cooling cycle with an ejector. Energy 2018;155:504-20.
844 [5] Li Y, An H, Li W, Zhang S, Jia X, Fu L. Thermodynamic, energy consumption and
845 economic analyses of the novel cogeneration heating system based on condensed waste
846 heat recovery. Energ Convers Manage 2018;177:671-81.
847 [6] Heng Z, Feipeng C, Yang L, Haiping C, Kai L, Boran Y. The performance analysis
848 of a LCPV/T assisted absorption refrigeration system. Renew Energ 2019;143:1852-64.
849 [7] Ochoa AAV, Dutra JCC, Henríquez JRG, dos Santos CAC, Rohatgi J. The influence
850 of the overall heat transfer coefficients in the dynamic behavior of a single effect
851 absorption chiller using the pair LiBr/H_2O. Energ Convers Manage 2017;136:270-82.
852 [8] Bellos E, Tzivanidis C, Tsifis G. Energetic, Exergetic, Economic and Environmental
853 (4E) analysis of a solar assisted refrigeration system for various operating scenarios.
854 Energ Convers Manage 2017;148:1055-69.
855 [9] Shokati N, Ranjbar F, Yari M. A comprehensive exergoeconomic analysis of
856 absorption power and cooling cogeneration cycles based on Kalina, part 1: Simulation.
857 Energ Convers Manage 2018;158:437-59.
858 [10] Shokati N, Ranjbar F, Yari M. A comprehensive exergoeconomic analysis of

absorption power and cooling cogeneration cycles based on Kalina, Part 2: Parametric study and optimization. Energ Convers Manage 2018;161:74-103.

[11] Novotny V, Vodicka V, Mascuch J, Kolovratnik M. Possibilities of water-lithium bromide absorption power cycles for low temperature, low power and combined power and cooling systems. Energy Procedia 2017;129:818-25.

[12] Rashidi J, Yoo CK. Exergetic and exergoeconomic studies of two highly efficient power-cooling cogeneration systems based on the Kalina and absorption refrigeration cycles. Appl Therm Eng 2017;124:1023-37.

[13] Rashidi J, Ifaei P, Esfahani IJ, Ataei A, Yoo CK. Thermodynamic and economic studies of two new high efficient power-cooling cogeneration systems based on Kalina and absorption refrigeration cycles. Energ Convers Manage 2016;127:170-86.

[14] Qu W, Su B, Tang S, hong H. Thermodynamic Evaluation of a hybrid solar concentrating photovoltaic/Kalina cycle for full spectrum utilization. Energy Procedia 2017;142:597-602.

[15] Qu W, Hong H, Su B, Tang S, Jin H. A concentrating photovoltaic/Kalina cycle coupled with absorption chiller. Appl Energ 2018;224:481-93.

[16] Al-Zareer M, Dincer I, Rosen MA. Multi-objective optimization of an integrated gasification combined cycle for hydrogen and electricity production. Comput Chem Eng 2018;117:256-67.

[17] De R, Bhartiya S, Shastri Y. Multi-objective optimization of integrated biodiesel production and separation system. Fuel 2019;243:519-32.

[18] Ehyaei MA, Ahmadi A, El Haj Assad M, Rosen MA. Investigation of an integrated system combining an Organic Rankine Cycle and absorption chiller driven by geothermal energy: Energy, exergy, and economic analyses and optimization. J Clean Prod 2020;258:120780.

884 [19] Asadi J, Amani P, Amani M, Kasaeian A, Bahiraei M. Thermo-economic analysis
885 and multi-objective optimization of absorption cooling system driven by various solar
886 collectors. Energ Convers Manage 2018;173:715-27.
887 [20] Li Y, Wang J, Zhao D, Li G, Chen C. A two-stage approach for combined heat and
888 power economic emission dispatch: Combining multi-objective optimization with
889 integrated decision making. Energy 2018;162:237-54.
890 [21] Konwar D, Gogoi TK, Das AJ. Multi-objective optimization of double effect series
891 and parallel flow water–lithium chloride and water–lithium bromide absorption
892 refrigeration systems. Energ Convers Manage 2019;180:425-41.
893 [22] Shirazi A, Taylor RA, Morrison GL, White SD. A comprehensive, multi-objective
894 optimization of solar-powered absorption chiller systems for air-conditioning
895 applications. Energ Convers Manage 2017;132:281-306.
896 [23] Cui P, Yu M, Liu Z, Zhu Z, Yang S. Energy, exergy, and economic (3E) analyses
897 and multi-objective optimization of a cascade absorption refrigeration system for low-
898 grade waste heat recovery. Energ Convers Manage 2019;184:249-61.
899 [24] Haghighat Mamaghani A, Najafi B, Shirazi A, Rinaldi F. 4E analysis and multi-
900 objective optimization of an integrated MCFC (molten carbonate fuel cell) and ORC
901 (organic Rankine cycle) system. Energy 2015;82:650-63.
902 [25] Jain V, Sachdeva G. Energy, exergy, economic (3E) analyses and multi-objective
903 optimization of vapor absorption heat transformer using NSGA-II technique. Energ
904 Convers Manage 2017;148:1096-113.
905 [26] Ameri M, Jorjani M. Performance assessment and multi-objective optimization of
906 an integrated organic Rankine cycle and multi-effect desalination system. Desalination
907 2016;392:34-45.
908 [27] Wang D, Feng X. Simulation and multi-objective optimization of an integrated

process for hydrogen production from refinery off-gas. Int J Hydrogen Energ 2013;38(29):12968-76.

[28] Ruiming F. Multi-objective optimized operation of integrated energy system with hydrogen storage. Int J Hydrogen Energ 2019;44(56):29409-17.

[29] Pourreza Movahed Z, Kabiri M, Ranjbar S, Joda F. Multi-objective optimization of life cycle assessment of integrated waste management based on genetic algorithms: A case study of Tehran. J Clean Prod 2020;247:119153.

[30] Hang Y, Du L, Qu M, Peeta S. Multi-objective optimization of integrated solar absorption cooling and heating systems for medium-sized office buildings. Renew Energ 2013;52:67-78.

[31] Gebreslassie BH, Guillén-Gosálbez G, Jiménez L, Boer D. Design of environmentally conscious absorption cooling systems via multi-objective optimization and life cycle assessment. Appl Energ 2009;86(9):1712-22.

[32] Li Y, Huang Y, Ye Q, Zhang W, Meng F, Zhang S. Multi-objective optimization integrated with life cycle assessment for rainwater harvesting systems. J Hydrol 2018;558:659-66.

[33] Gao S, Bo C, Li J, Niu C, Lu X. Multi-objective optimization and dynamic control of biogas pressurized water scrubbing process. Renew Energ 2020;147:2335-44.

[34] Liu Z, Xie N, Yang S. Thermodynamic and parametric analysis of a coupled $LiBr/H_2O$ absorption chiller/Kalina cycle for cascade utilization of low-grade waste heat. Energ Convers Manage 2020;205:112370.

[35] He J, Liu C, Xu X, Li Y, Wu S, Xu J. Performance research on modified KCS (Kalina cycle system) 11 without throttle valve. Energy 2014;64:389-97.

[36] Cao L, Wang J, Wang H, Zhao P, Dai Y. Thermodynamic analysis of a Kalina-based combined cooling and power cycle driven by low-grade heat source. Appl Therm

934 Eng 2017;111:8-19.
935 [37] Akbari Kordlar M, Mahmoudi SMS, Talati F, Yari M, Mosaffa AH. A new flexible
936 geothermal based cogeneration system producing power and refrigeration, part two:
937 The influence of ambient temperature. Renew Energ 2019;134:875-87.
938 [38] Jing X, Zheng D. Effect of cycle coupling-configuration on energy cascade
939 utilization for a new power and cooling cogeneration cycle. Energ Convers Manage
940 2014;78:58-64.
941 [39] Wang J, Wang J, Zhao P, Dai Y. Thermodynamic analysis of a new combined
942 cooling and power system using ammonia–water mixture. Energ Convers Manage
943 2016;117:335-42.
944 [40] Seckin C. Thermodynamic analysis of a combined power/refrigeration cycle:
945 Combination of Kalina cycle and ejector refrigeration cycle. Energ Convers Manage
946 2018;157:631-43.
947 [41] Yang S, Wang Y, Gao J, Zhang Z, Liu Z, Olabi AG. Performance Analysis of a
948 Novel Cascade Absorption Refrigeration for Low-Grade Waste Heat Recovery. ACS
949 Sustain Chem Eng 2018;6(7):8350-63.
950 [42] Yang S, Yang S, Wang Y, Qian Y. Low grade waste heat recovery with a novel
951 cascade absorption heat transformer. Energy 2017;130:461-72.
952 [43] Yang S, Qian Y, Wang Y, Yang S. A novel cascade absorption heat transformer
953 process using low grade waste heat and its application to coal to synthetic natural gas.
954 Appl Energ 2017;202:42-52.
955 [44] Ma X, Chen J, Li S, Sha Q, Liang A, Li W, et al. Application of absorption heat
956 transformer to recover waste heat from a synthetic rubber plant. Appl Therm Eng
957 2003;23(7):797-806.
958 [45] Smith R. Chemical Process Design and Integration, 2nd Edition: John Wiley &

959 Sons Ltd, 2016.
960 [46] CHEMICAL ENGINEERING PLANT COST INDEX: 2018 ANNUAL VALUE.
961 2019. URL: https://www.chemengonline.com/2019-cepci-updates-january-prelim-and-
962 december-2018-final/
963 [47] Goedkoop M, Spriensma R. The Eco-Indicator 99: A Damage Oriented Method
964 for Life Cycle Impact Assessment. Amersfoort, The Netherlands: PRé Consultants b.v.,
965 2001.
966 [48] Guillén-Gosálbez G, Caballero JA, Esteller LJ, Gadalla M. Application of life
967 cycle assessment to the structural optimization of process flowsheets. Comput Aided
968 Chem Eng 2007;24:1163-8.
969 [49] Song R, Cui M, Liu J. Single and multiple objective optimization of a natural gas
970 liquefaction process. Energy 2017;124:19-28.
971 [50] Luo Z, Yang S, Xie N, Xie W, Liu J, Souley Agbodjan Y, et al. Multi-objective
972 capacity optimization of a distributed energy system considering economy,
973 environment and energy. Energ Convers Manage 2019;200:112081.
974 [51] Li C, Bai H, Lu Y, Bian J, Dong Y, Xu H. Life-cycle assessment for coal-based
975 methanol production in China. J Clean Prod 2018;188:1004-17.
976